

## A SHASHLIK CALORIMETER WITH LONGITUDINAL SEGMENTATION FOR A LINEAR COLLIDER

I. Britvich, A. Feniouk, V. Lishin, V. Obraztsov, V. Poliakov, E. Vlasov  
*Institute for High Energy Physics, Serpukov, Russia*

T. Camporesi, L. Masetti, F. Marcucci, E. Piotto  
*CERN, European Organization for Nuclear Research, Geneva, Switzerland*

S. Ask, V. Hedberg  
*Department of Physics, University of Lund, Lund, Sweden*

M. Paganoni, F. Terranova  
*Dipartimento di Fisica, Università di Milano Bicocca and INFN, Milan, Italy*

P. Checchia, M. Margoni, M. Mazzucato, F. Simonetto  
*Dipartimento di Fisica, Università di Padova and INFN, Padua, Italy*

Presented by: P. Checchia

### ABSTRACT

Two techniques for longitudinal segmentation of Shashlik calorimeter are proposed and tested in order to prove the feasibility of an ElectroMagnetic calorimeter based on the Shashlik technology for a detector at a future Linear Collider. Results concerning energy resolution and  $e/\pi$  separation are reported.

### 1 Introduction

In recent years the “Shashlik” technology has been extensively studied to assess its performance at  $e^+e^-$ ,  $ep$  and  $pp$  accelerator experiments <sup>1)- 4)</sup>. Shashlik calorimeters are sampling calorimeters in which scintillation light is read-out via wavelength shifting (WLS) fibers running perpendicularly to the converter/absorber plates <sup>5, 6)</sup>. This technique offers the combination of an easy

assembly, good hermeticity and lower cost as compared to crystals or cryogenic liquid calorimeters.

Shashlik calorimeters are good candidates for barrel electromagnetic calorimetry at future linear  $e^+e^-$  colliders <sup>7)</sup> because they satisfy the requirements of very high granularity with a transversal segmentation of the order of  $0.9^\circ \times 0.9^\circ$  ( $\sim 3 \times 3 \text{ cm}^2$ ), fairly good energy resolution ( $\sigma(E)/E \leq 0.15/\sqrt{E(\text{GeV})} + 0.01$ ) and compactness (25-30  $X_0$  in 25-30 cm). They can furthermore be operated inside a high 4 T magnetic field. A longitudinal segmentation however is essential for a good  $e/\pi$  separation, and needs to be studied and implemented.

The CALEIDO collaboration has proposed and tested two solutions for longitudinal segmentation:

1) the insertion of thin vacuum photodiodes (5 mm) between adjacent towers in the front part of the calorimeter (CALEIDO1);

2) the use of a slow ( $\tau \simeq 250 \text{ ns}$ ) scintillator as sampling medium in the front part of the calorimeter, combined with a fast scintillator in the rest of the detector (CALEIDO2).

## 2 CALEIDO1

A prototype detector was exposed to a beam with the aim of measuring the sampling capability and demonstrating that the insertion of diodes neither deteriorates critically the energy response nor produces significant cracks in the tower structure. The prototype had 25 Pb/scintillator towers, assembled in a  $5 \times 5$  matrix. Each tower consisted of 140 layers of 1 mm thick lead and 1 mm thick scintillator tiles, resulting in a total depth of  $25X_0$ . The transversal dimension of each tower was  $5 \times 5 \text{ cm}^2$ . Plastic scintillator consisting of polystyrene doped with 1.5% paraterphenyl and 0.05% POPOP was used. Optical insulation between the towers was provided by white Tyvek paper.

The blue light produced in the scintillator was carried to the photodetector at the back of the calorimeter by means of plastic optical fibers doped with green WLS. The 1 mm diameter fibers crossed the tiles in holes drilled in the lead and scintillator plates and they were uniformly distributed with a density of 1 fiber/ $\text{cm}^2$ . All the fibers from the same tower were bundled together at the back and connected to photodetectors (1" Hamamatsu R2149-03 phototetrodes). In the first  $8X_0$  the tiles had a smaller transverse dimension to provide room for the housing of the diodes ( $9 \times 5 \times 0.5 \text{ cm}^3$  EMI vacuum pho-

todiode prototype D437 and  $5 \times 5 \times 0.5 \text{ cm}^3$  Hamamatsu vacuum photodiode prototype SPTXC0046).

A very good  $e/\pi$  separation ( $< 5 \times 10^{-4}$  at 50 GeV) was achieved and an energy resolution

$$\frac{\sigma(E)}{E} = \sqrt{\left(\frac{9.6\%}{\sqrt{E}} + 0.5\%\right)^2 + \left(\frac{0.130}{E}\right)^2} \quad (1)$$

where  $E$  is expressed in GeV was obtained. The position resolution of the prototype at the cell center was 1.6 mm with 50 GeV electrons.

A detailed discussion of the results can be found in <sup>8)</sup>.

In order to study the feasibility of a calorimeter with higher granularity ( $3 \times 3 \text{ cm}^2$  lateral cell size), a smaller vacuum photodiode ( $5 \times 3 \times 0.5 \text{ cm}^3$  Hamamatsu prototype PPTXC00052) was tested. The energy response to the early shower development of 30 and 50 GeV electron beam is shown in fig. 1.

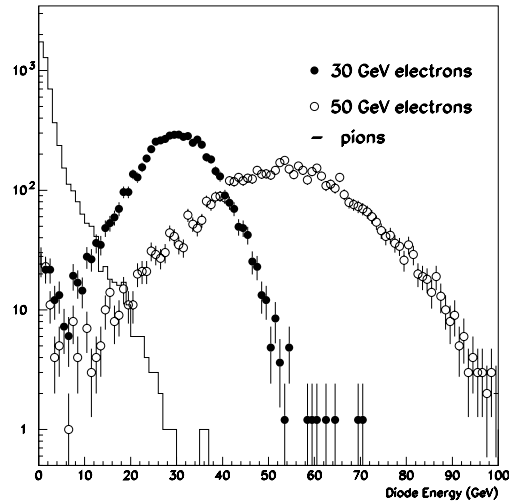


Figure 1: *Energy response for 30 and 50 GeV electrons and for 30 GeV pions for the  $5 \times 3 \times 0.5 \text{ cm}^3$  Hamamatsu photodiode.*

### 3 CALEIDO2

The second prototype had 9 Pb/scintillator towers ( $5 \times 5 \times 28 \text{ cm}^3$ ) assembled in a  $3 \times 3$  matrix. In each tower, the scintillator Bicron BC-444, characterized

by a decay time of about 250 ns, was used in the first 29 layers (corresponding to the first 5  $X_0$ ). Its decay time is much longer than the the decay time of the CALEIDO1 scintillator which is faster than 10 ns, and which was used in the residual 100 layers of CALEIDO2. The light produced in each tower by both the fast and the slow scintillator was carried to the same photodetector by means of KY11 fibers. These are fast enough not to deteriorate the separation between the fast and the slow scintillator signals. Various photomultipliers were tested in order to optimize the separation between the fast and the slow scintillator signals. Fig. 2 shows the time response to the fast scintillator signal for the photomultipliers FEU 84-3 and FEU 115-M. FEU 84-3 was used in a 1999 run at the X7 CERN West Area beam while the latter was chosen for the 2000 test in the H6 CERN Nord Area beam line.

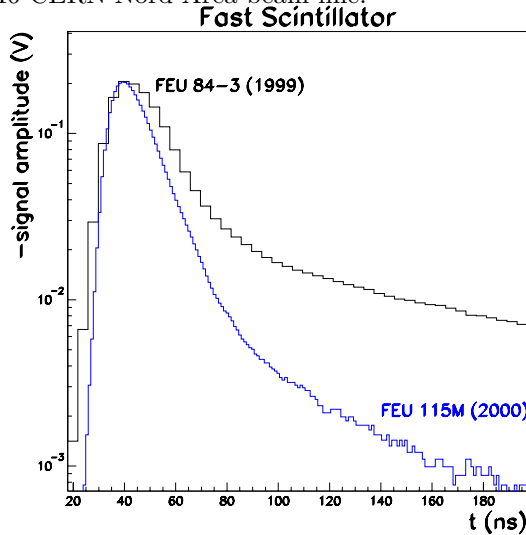


Figure 2: Time profile of the signals from FEU 84-3 and FEU 115-M photomultipliers for a fast scintillator.

The read-out was performed by splitting the signal in two by means of a passive splitter and by sampling with two differently gated ADC's. The first gate (referred to in the following as the narrow gate) was 50 ns wide. It started at the signal front rise in order to convert mainly the fast component. The second gate (referred to in the following as the wide gate) had a 50 ns delay with respect to the narrow gate and it was 150 ns wide in order to convert a

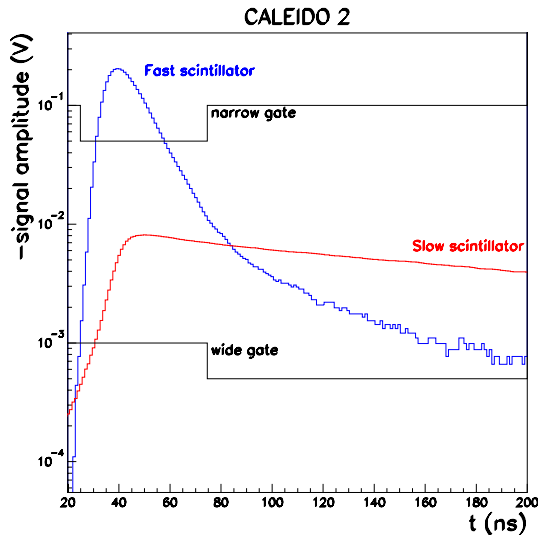


Figure 3: *Time profile of the signals from fast and slow scintillator for FEU 115-M photomultiplier. The narrow and wide gates are also showed.*

large fraction of the long decay time component (see fig. 3).

In order to analyze the data of the CALEIDO2 prototype the energies deposited in the slow ( $E_{slow}$ ) and in the fast ( $E_{fast}$ ) scintillator had to be extracted from the ADC values of the wide ( $Q_w$ ) and narrow ( $Q_n$ ) gates. In fig. 4, which shows the correlation between  $Q_w$  and  $Q_n$  for electrons and pions at 50 GeV, it is evident that a fraction of the signal from the fast component is sampled also by the wide gate. Therefore a linear transformation had to be made in order to obtain  $E_{slow}$  and  $E_{fast}$  from  $Q_w$  and  $Q_n$ . (fig. 4). The two scintillators had furthermore different light yields and, after a cross calibration of the two components, the resolution improves, as it is shown in fig. 5.

From a preliminary analysis of the data collected in the 2000 runs the energy resolution can be parametrized (see fig. 6) as a function of the beam energy by:

$$\frac{\sigma(E)}{E} = \frac{14.2\%}{\sqrt{E}} + 0.6\% \quad (2)$$

The signal extracted from the slow component versus the total energy is shown in fig. 7 for 30 GeV electrons and pions. The discriminating power of

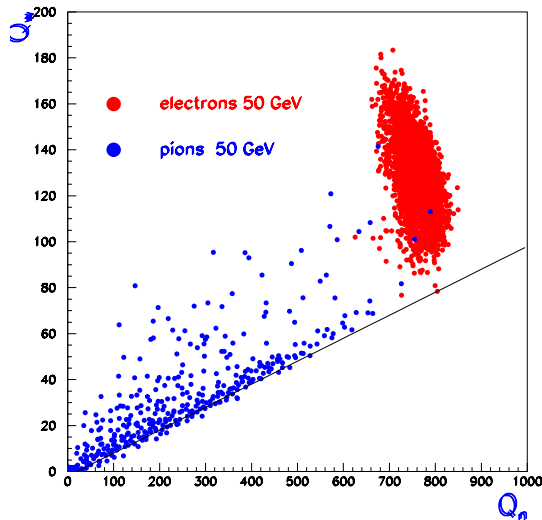


Figure 4: Signal collected in the wide gate versus the signal collected in the narrow gate for 50 GeV electrons and pions. The line corresponds to the contribution to the wide gate signal attributed to the fast scintillator.

the  $E_{slow}$  information (fig. 8) improves the separation capability by a factor  $\sim 2$  w.r.t. the E/p ratio. These results agree with the results from the 1999 data taking <sup>9)</sup> and prove the technical feasibility of the proposed method.

#### 4 A detector for a Linear Collider

Since both the proposed techniques work, a Shashlik electromagnetic calorimeter is a good candidate for a detector at a future Linear Collider. The second technique proposed here, despite of the worse energy resolution, offers mechanical advantages. In particular a lateral granularity of  $\sim 3 \times 3$  cm<sup>2</sup> can be obtained in a simple way by using large (i.e.  $\sim 20 \times 10$  cm<sup>2</sup>) absorber plates and confining the scintillation light inside the defined granularity region. This scheme substitutes the small tower structure which is unavoidable if the lateral diode has to be inserted. In the TESLA TDR <sup>10)</sup> a Shashlik solution is proposed for a barrel electromagnetic calorimeter based on  $19.2 \times 10$  cm<sup>2</sup> lateral size modules each with 18 channels having two decay-time scintillators.

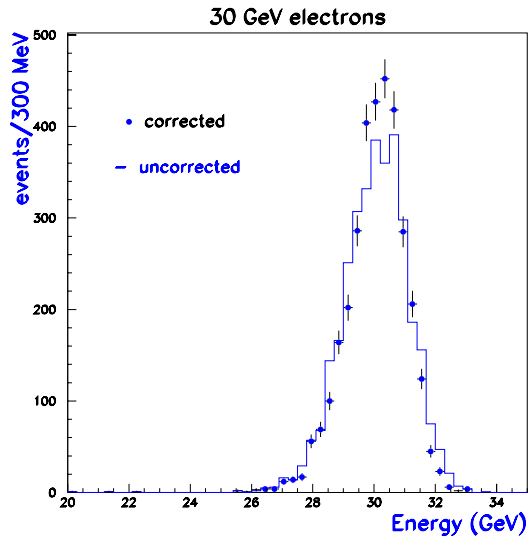


Figure 5: Energy resolution, for 30 GeV electrons, before and after calibration between the slow and the fast scintillator.

## 5 Conclusions

Beam tests have demonstrated the technical feasibility of longitudinally segmented shashlik calorimeters in which longitudinal sampling is performed by lateral vacuum photodiodes or by using two scintillator types with different decay times. Performance in terms of energy resolution, impact point reconstruction and  $e/\pi$  separation are adequate for applications at future  $e^+e^-$  collider experiments.

## References

1. J. Badier *et al.*, Nucl. Instr. and Meth. **A348** (1994) 74.
2. HERA-B Design report, DESY/PRC 95-01.
3. LHCb Technical proposal, CERN/LHCC 98-4.
4. S.J. Alsvaag *et al.*, CERN/EP 98-132.
5. H. Fessler *et al.*, Nucl. Instr. and Meth. **A240** (1985) 284.

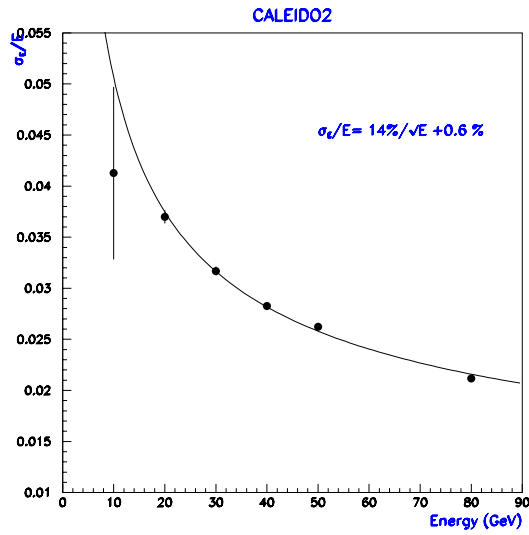


Figure 6: *Energy resolution as function of the electron energy.*

6. G.S. Atoyan *et al.*, Nucl. Instr. and Meth. **A320** (1992) 144.
7. R. Brinkmann, G. Materlik, J. Rossbach, A. Wagner (eds.), DESY 1997-048.
8. A.C. Benvenuti *et al.*, Nucl. Instr. and Meth. **A432** (1999) 232-239.
9. A.C. Benvenuti *et al.*, iee Transaction in Nuclear Science, in publication.
10. TESLA TDR in preparation.



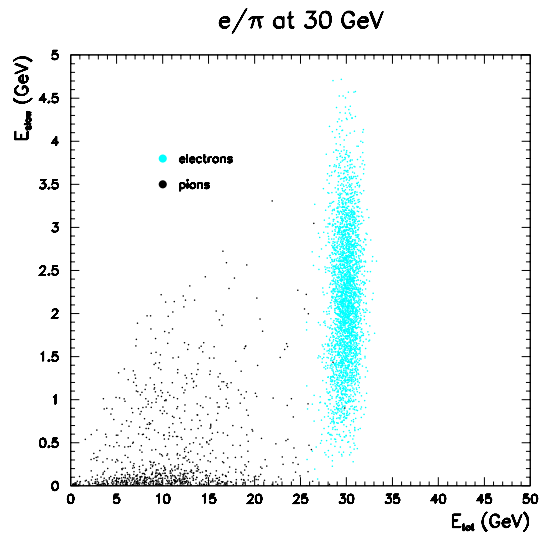


Figure 7: *CALEIDO2*: slow scintillator energy versus total energy for  $e$  and  $\pi$  at 30 GeV.

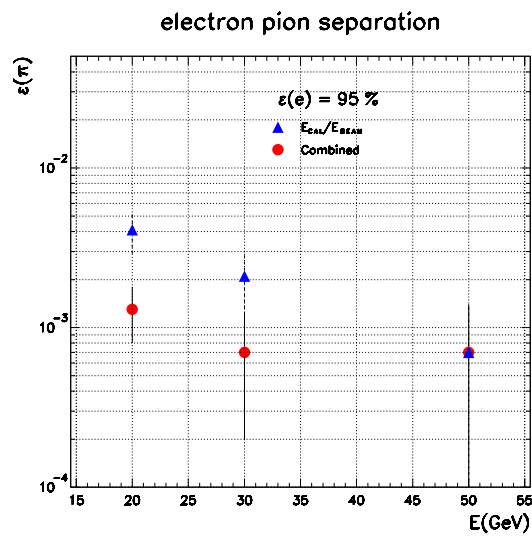


Figure 8: Pion contamination versus energy for 95% electron efficiency.